LA-UR- 09-08244

*Approved for public release; distribution is unlimited.*

| | |
|---|---|
| *Title:* | Non-Equilibrium Molecular Dynamics and Dynamic Deformation at Sliding Metal-Metal Interfaces |
| *Author(s):* | Hammerberg, James E.; Holian, Brad, L.; Germann, Timothy C.; Ravelo, Ramon, J. |
| *Intended for:* | International Symposium on Plasticity 2010; St. Kitts, West Indies |

Los Alamos
NATIONAL LABORATORY
EST. 1943



Form 836 (7/06)

# Non-Equilibrium Molecular Dynamics and Dynamic Deformation at Sliding Metal-Metal Interfaces

**J.E. Hammerberg, B.L.Holian, T.C.Germann and R. Ravelo**

**Los Alamos National Laboratory**

**January 5, 2010**

**International Symposium on Plasticity 2010**

**St. Kitts, West Indies**

**January 3-8, 2010**

LA-UR-09-xxxxx

# Overview

- Experimental background for metal-metal sliding
- Large-scale Non-Equilibrium Molecular Dynamics (NEMD) simulations to characterize physical mechanisms
- Generic properties of the velocity dependence of the frictional force
- Summary

# Experimental Overview – Velocity Dependence

- **High speed levitated sphere experiments of Bowden and collaborators demonstrated significant weakening of the frictional force with increasing velocities to 700 m/s**

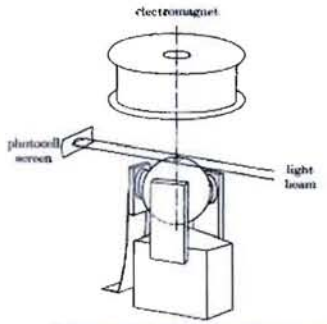


FIGURE 1. Schematic diagram of high-speed friction apparatus.

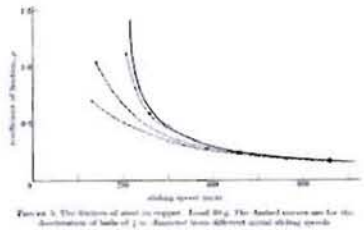

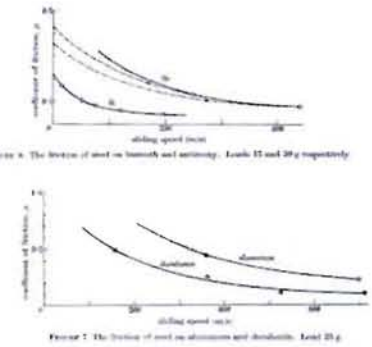

Bowden, F.P. and Freitag, E.H., 1958, "The Friction of Solids at Very High Speeds", Proc. Roy. Soc. (Lond) Ser. A, Vol. 248, pp. 350-367.

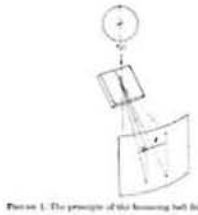

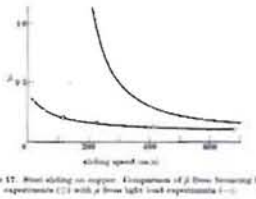

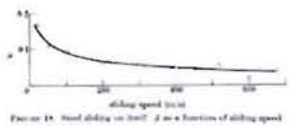

Bowden, F.P. and Persson, P.A., 1961, "Deformation, Heating and Melting of Solids in High-Speed Friction", Proc. Roy. Soc. (Lond.) Ser. A, Vol. 260, pp. 433-458.

# Experimental Overview – Velocity Dependence

**ATLAS pulsed power experiments measured similar velocity weakening at a Ta/Al interface at 15 GPa for Sliding velocities between 360 and 700 m/s**

- Hollow, cylindrical "lifesaver" sandwich target enabled diagnostic access and reduced end effects
- Low $C_s$ material (Ta)
- High $C_s$ material (Al)
- Low $C_s$ material (Ta)
- 2-interfaces/experiment (2/6 μm RMS finish)
- Thick liner (7 mm initial, 10 mm at impact)
- maintained shocked state longer
- produced greater interface displacement
- Must be transparent to radiography
- 1.5 - 2.5 km/s impact velocity

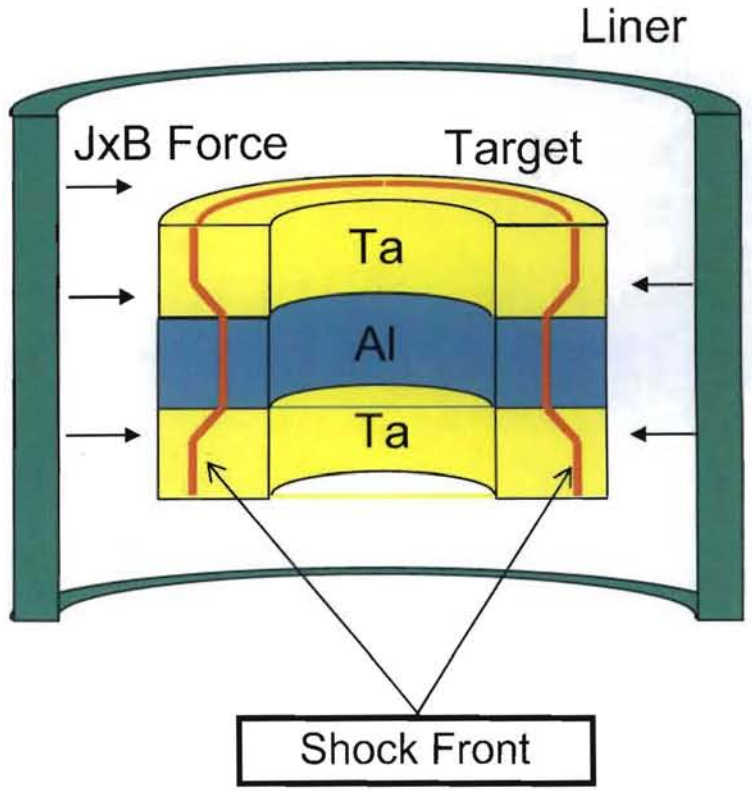


**[C.A. Rousculp et al., "Dynamic Friction Experiments at the ATLAS Pulsed Power Facility", Proc. 2006 Int. Conf. on MegaGauss Magnetic Field Generation and Related Topics, 2007.]**

# Experimental Overview – Velocity Dependence

**Atlas Pulsed Power Facility at NTS Provided Reproducible, Tunable Drive**

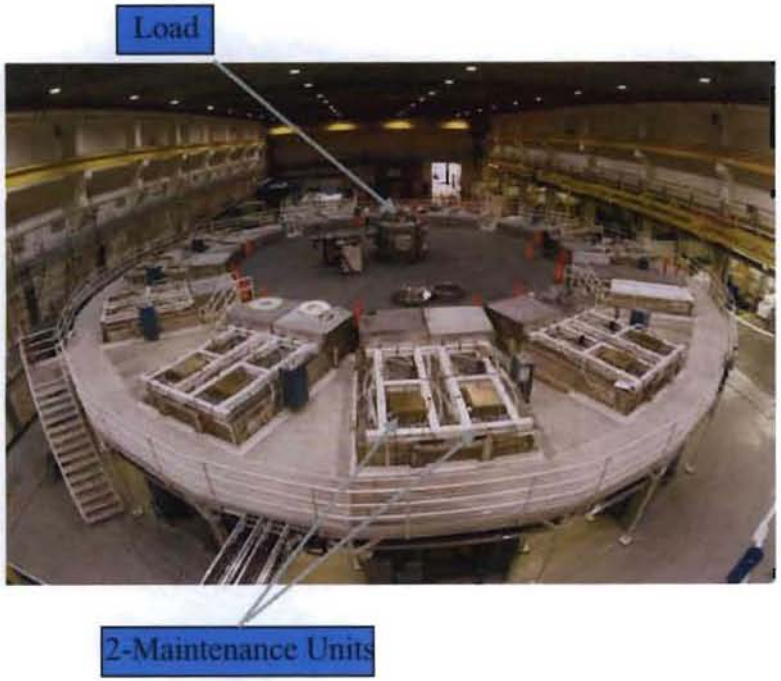


- 26 MJoules stored energy, 6 ms rise time
- Symmetric, cylindrically converging geometry
- 1/3, 2/3, 3/3 bank configurations (and others)

# Experimental Overview – Velocity Dependence

- Transverse radiography measured bending of 0.4mm Au wires. Lagrangian analysis determines F/A

Static Pre-shot Radiograph

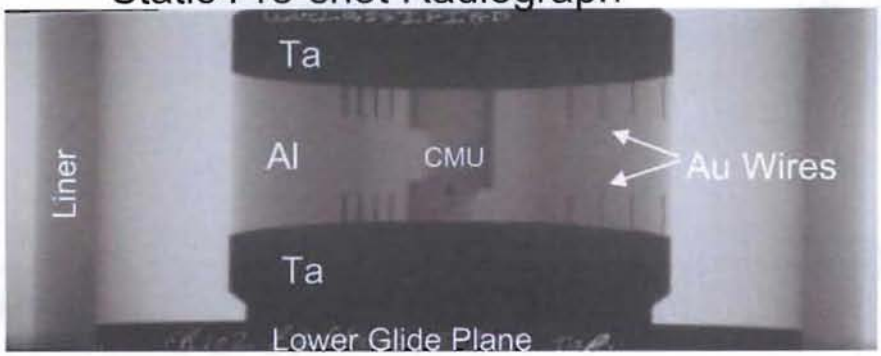


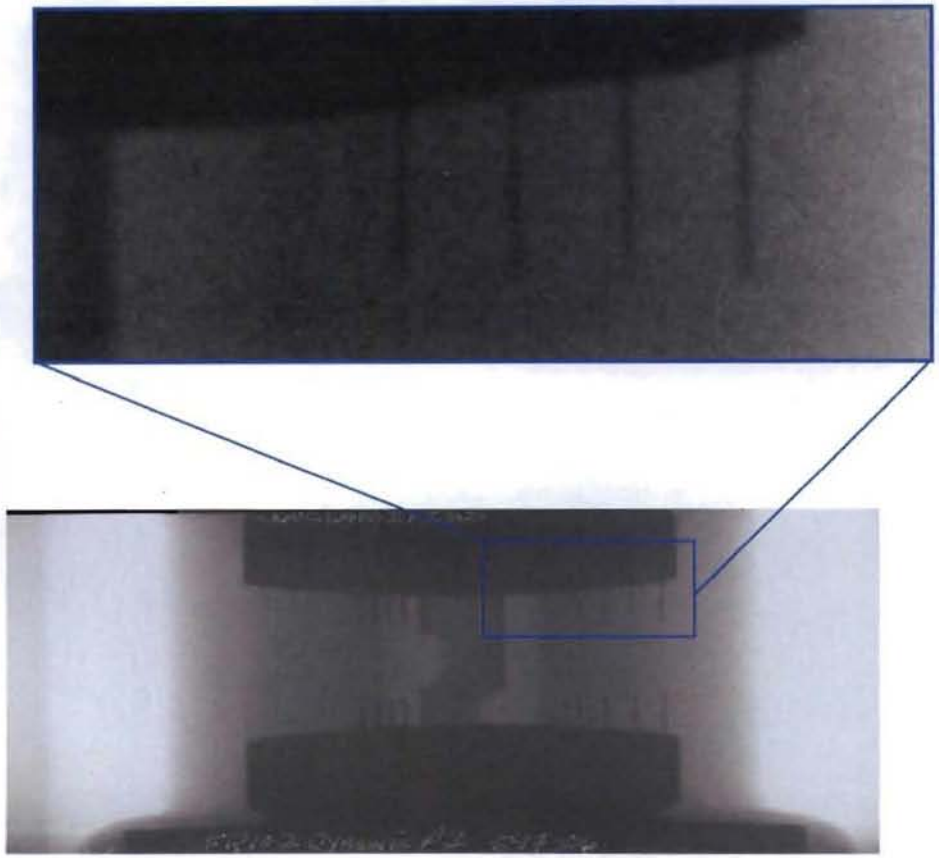

Dynamic Radiograph (t = 22.2 μs )

# Experimental Overview – Velocity Dependence

- Lagrangian analysis showed velocity weakening

| Expt. | $V_{impact}$ (mm/μs) | P (GPa) | Δt (μs) | $F_{tang}/A$ (GPa) | Yield Strength (GPa) | $\langle v_{int} \rangle$ (mm/μs) |
|---|---|---|---|---|---|---|
| FR 102 | 1.3 | 13 | 3.58 | 0.60 | 0.8 | 0.36 |
| FR 103 | 1.5 | 15 | 3.727 | 0.09 | 0.9 | 0.56 |
| FR 101 | 1.7 | 18 | 2.408 | < 0.09 | 1.0 | 0.70 |

# Experimental Overview – Velocity Dependence

- **Explosively driven experiments**


Figure 2. The FN6 experiment. The aluminium (top) and stainless steel (bottom) components were machined to a surface roughness of 3.2 μm and were flat such that the maximum gap that could exist between the sliding surfaces was <25 μm. The components were held in contact by gravity.

Figure 6. The steel component recovered from FN6-3-3. The outlines of the surface markings mirror the corresponding outlines on the aluminium block (see figure 5).

[R.E. Winter et al., 2006, "Mechanisms of Shock-Induced Dynamic Friction", J.Phys. D, Vol. 39, pp. 5043-5053

- **Rotating Barrel Gas Gun**

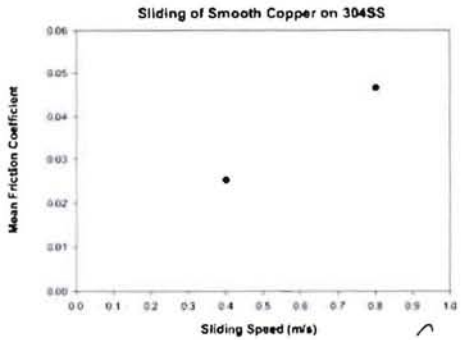


[P. Crawford et al.,2003, "A Novel Experimental Technique for the Study of High-Speed Friction under Elastic Loading Conditions", Proc. Shock Compression of Condensed Matter – 2003, pp. 545-548]

# Experimental Overview – Velocity Dependence

- **Plate-Impact pressure-shear friction experiment**

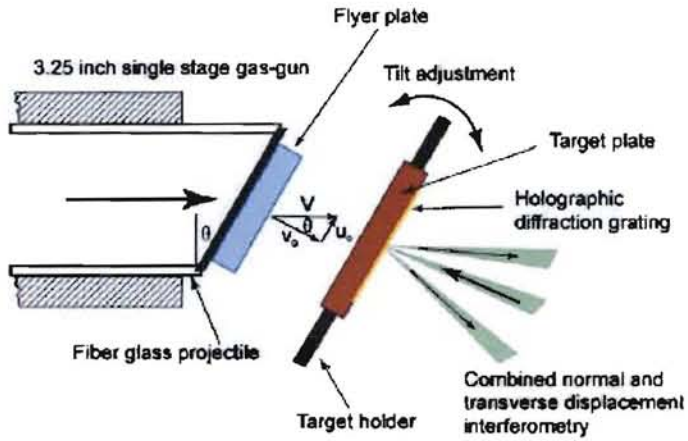


Fig. 1. Schematic of the plate-impact pressure-shear friction experiment.

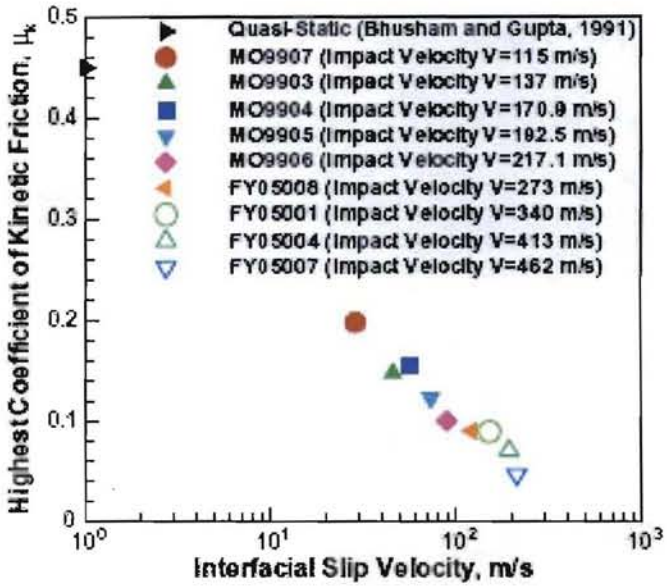


[F. Yuan, N.-S. Liou and V. Prakash, 2009, "High-Speed Frictional Slip at Metal-on-Metal Interfaces", Int. J. Plast., Vol. 25, pp. 612-634.]

# Experimental Overview – Structural Transformation

- **Dry sliding induces subgrain nanostructure and highly strained graded microstructure in ductile metals**

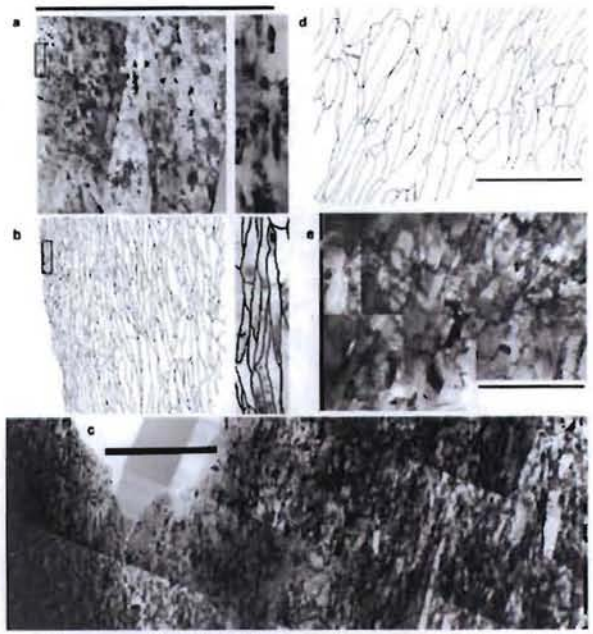

FIG. 1. Graded nanostructures produced by friction deformation as viewed in cross section by TEM. (a) Micrograph and (b) tracing of extended boundaries in Cu following sliding under 12 MPa applied normal pressure, the left side is coincident with the surface. Rectangular boxes show location of the adjacent high magnification excerpts illustrating a layer with 12 nm average boundary spacing. These rectangles are 70 nm wide. (c) Following sliding with 22 MPa pressure, the surface is coincident with the left side. (The pale gray regions underneath the scale marker is the hole produced when making the TEM foil.) (d) Tracing and micrograph (e) of sample in (a) but at 20 μm below the surface. Scale markers are 2 μm.

**[D.A. Hughes and N. Hansen, 2001, "Graded Nanostructures Induced by Sliding and Exhibiting Universal behavior", Phys. Rev. Lett. Vol. 87, pp. 1355031-1355034.]**

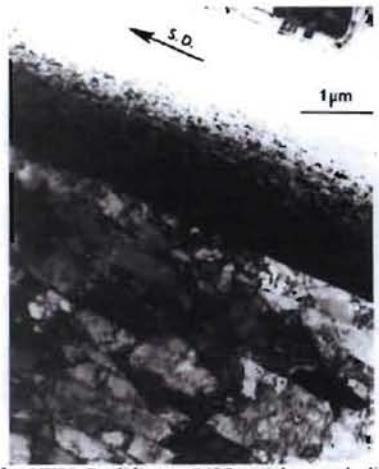


Figure1: TEM micrograph for OFHC Cu sliding on 440C stainless steel, sliding at 1 cm/sec for 12 m at normal load 66.6 . Longitudinal section. Arrow denotes sliding direction. From Ref. (22).

**[D.A. Rigney, 19887, "Sliding Wear of Metals", Ann. Rev. Mater. Sci., Vol. 18, pp. 141-163.]**

# Experimental Overview – Structural Transformation

- **Cu pin on disk and Al explosively driven experiments show nanocrystalline regions and highly strained regions at the sliding interface**


Fig. 4. FIB ion channeling images of transverse cross-sections from the disk wear track showing (a) a gradient of increasing grain sizes below the wear track for a 0.25 m/s test and (b) the abrupt transition from a subsurface nanocrystalline region to a large grained region for a 1.5 m/s test.

[Andrew Emge, S. Karthikeyan, H.J. Kim and D.A. Rigney, 2007, "The Effect of Sliding Velocity on the Tribological Behavior of Copper", Wear, Vol. 263, pp. 614-618]

Fig. 8. TEM micrograph of a cross-section of tested AW5083 aluminum. A thin nanocrystalline layer (left side) and adjacent heavily deformed material are shown. The resolution of the structure is higher here than in Fig. 7. Using both types of images provides the desired resolution and demonstrates that the structures are not simply local effects.

[H.J. Kim, A. Emge, R.E. Winter, P.T. Keightley, W.J. Kim, M.L. Falk, and D.A. Rigney, 2009, "Nanostructures generated by Explosively Driven Friction: Experiments and Molecular Dynamics Simulations", Acta Mater. doi:10.1016/j.actamat.2009.07.034]

# Experimental Overview – Material Mixing

- **Nanocrystalline mixing layer (A) at a Cu/SS interface**

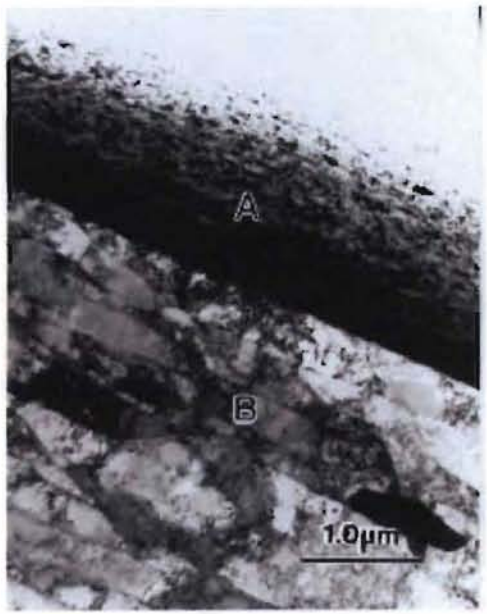


Fig. 3. TEM image of longitudinal section of OFHC copper block a:
:er sliding against 440°C steel ring. Note sharp demarcation betwee
nanocrystalline mixed material and deformation substructure (subgrain
of base material. Same sample and conditions as in Fig. 1.

**[D.A. Rigney, 2000, "Transfer, Mixing and Associated Chemical and Mechanical Processes During the Sliding of Ductile Metals", Wear, Vol. 245, pp. 1-9.]**

# Summary - Experimental

- Frictional force at metal-metal interfaces exhibits a decrease with increasing sliding velocity at high velocities (velocity weakening).
- The near surface microstructure transforms to smaller length scale structure which is graded and exhibits very high plastic strains in regions of tens of microns from the sliding interface.
- There is evidence for a mechanically mixed layer of nanoscale material at the sliding interface.

# Large-Scale NEMD Simulations of the tangential force as a function of sliding velocity and compression

- Experimental data for the tangential force as a function of velocity and compression are sparse and difficult to obtain dynamically.
- Integral experiments have been carried out by R. Winter et al. using high explosive drive. Pulsed power radiographic experiments have also been carried out (G. Kyrala, R. Faehl, C. Rousculp et al. LANL – Pegasus, Atlas experiments) which are more nearly direct measurements of the tangential force.
- Rotating Barrel Gas Gun experiments (P.Rightley, P.Crawford and K. Rainey, LANL) allow measurements of $F_t$ at velocities less than 100 m/s. Pressure-shear measurements have been been carried out to 450 m/s (v. Prakash et al.).
- Large scale NonEquilibrium Molecular Dynamics (NEMD) allow for microscopic interrogation of physical mechanisms at relevant sliding rates (0 – 1 km/s).

# NEMD Simulations

**A simulation strategy was formulated to understand the underlying physical mechanisms using a particular Boundary condition.**

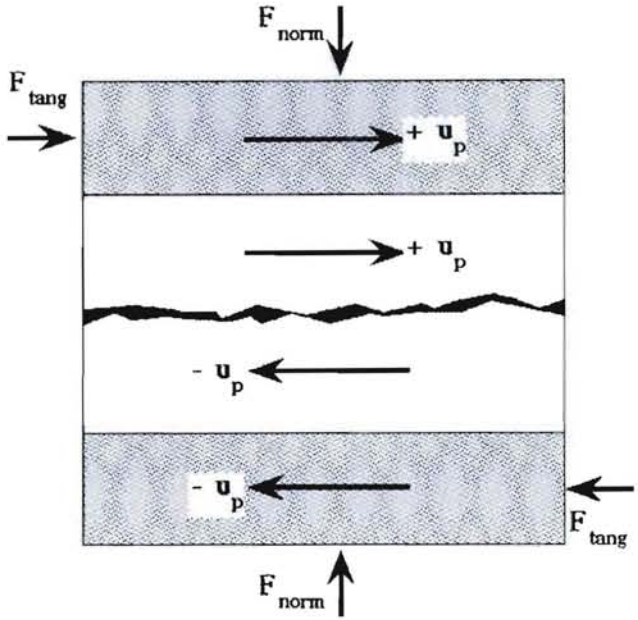


**Typical system sizes: $10^6$ atoms**
**Typical integration times: 1 ns**


[J.E.Hammerberg, B.L. Holian, J. Roeder, A.R. Bishop and S.J. Zhou, 1998, "Nonlinear dynamics and the problem of slip at material interfaces", Physica D, Vol. 123, pp. 330-340.
J.E. Hammerberg and B.L. Holian, 2004, "Simulation Methods for Interfacial Friction in Solids", in Surface Modification and Mechanisms, G.E. Totten and H. Liang, eds., pp.723-749.]

# NEMD Simulations

- **Initial Cu/Cu two dimensional simulations showed all three experimental features: velocity weakening, structural transformation and mechanical mixing.**

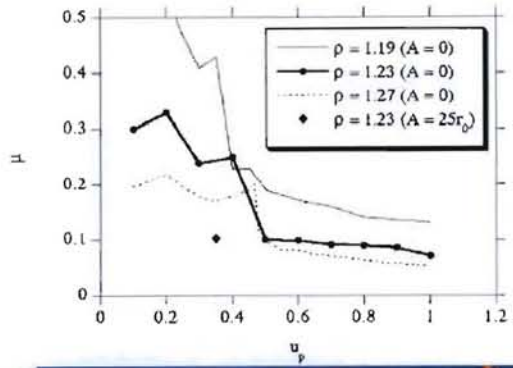


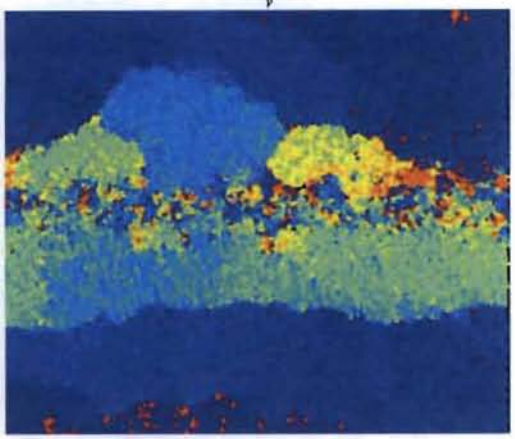

**Cu(2D) Grain Structure**

**Cu(2D) P=30GPa, v- 0.12$c_t$, Mechanical Mixing**

Evolution of mixed layer

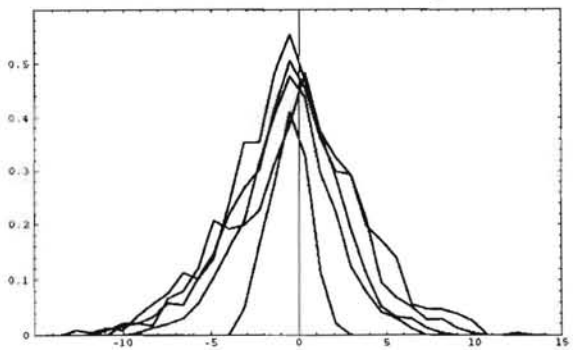

times: 100,200,300,400,500 $t_0$

# Material pairs investigated with NEMD

**Material pairs investigated:**

| Tribo-Pair | Dimension | $V_{max}$ ($cm\mu s^{-1}$) | $P_{max}$ (GPa) |
|---|---|---|---|
| Cu/Cu | 2 | 0.30 | 30 |
| L-J/L-J | 2 | 0.25* | 10.0 |
| Cu/Ag | 3 | 0.12 | 5 |
| Ta/Al | 3 | 0.30 | 15 |
| Al/Al | 3 | 0.30 | 15 |

*For the Lennard-Jones system velocities and pressures are given in Lennard-Jones units.

# Velocity Dependence: Generic properties of high velocity sliding

**There is a variety of experimental evidence that at high velocities the frictional force decreases with increasing velocity. | cf. J.E. Hammerberg and B.L.Holian, "Simulation Methods for Interfacial Friction in Solids" in Surface Modification and Mechanisms, 2004 (G.E.Totten and H.Liang, eds.) pp.723-749]. The figure below shows simulation results for an Al(111)/Al(001) interface.**

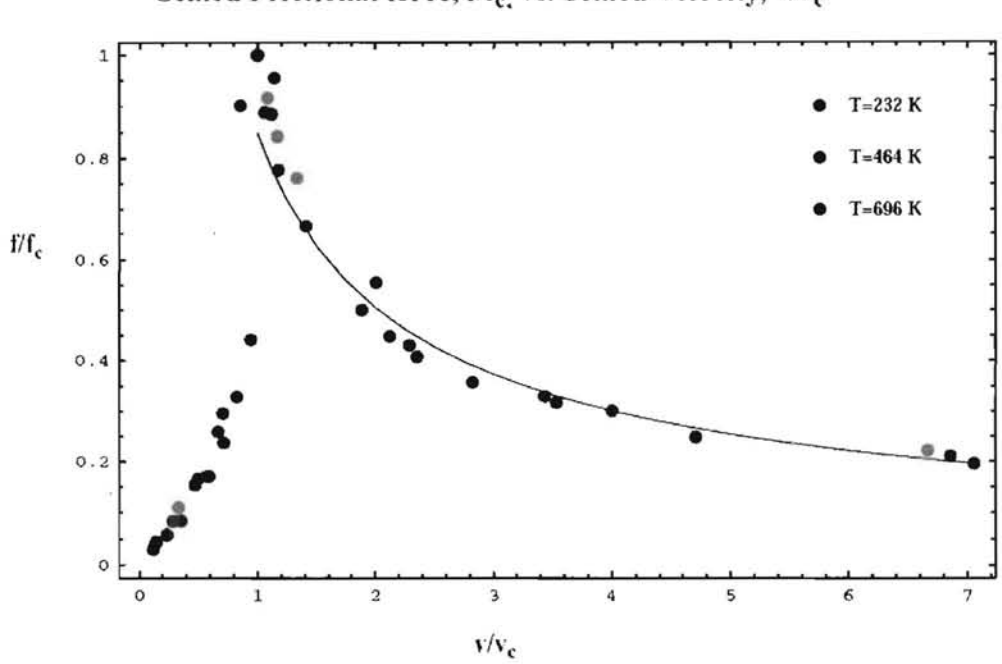

# Velocity Dependence: Lennard-Jones (2D) and Cu/Ag (3D) Interfaces

**Tangential force vs. sliding velocity**

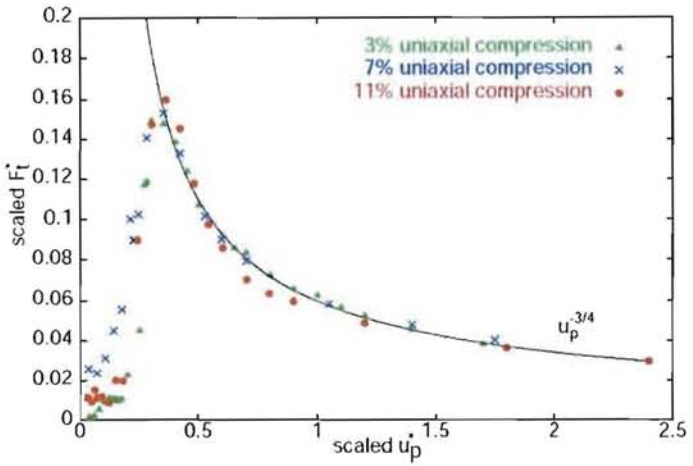


Scaled tangential force for a flat 2-D Lennard-Jones solid incommensurate interface at three compressions. The high velocity behavior scales as $v^{-b}$ with b=3/4.

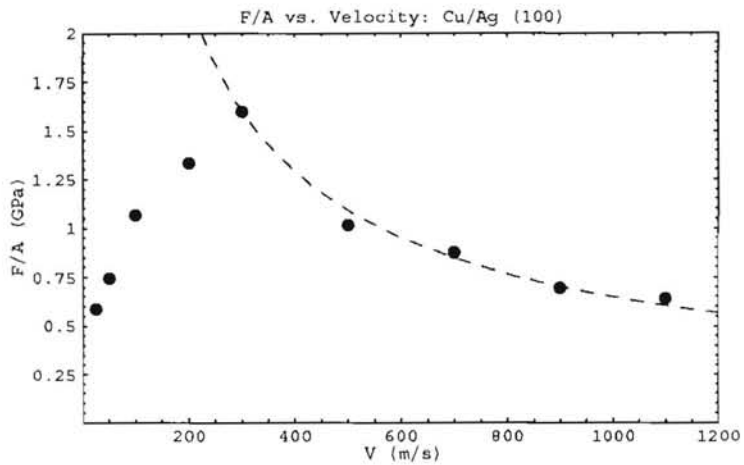


Cu/Ag (5 GPa)

# Velocity Dependence: Ta/Al (3D) and Al/Al (3D) Interfaces

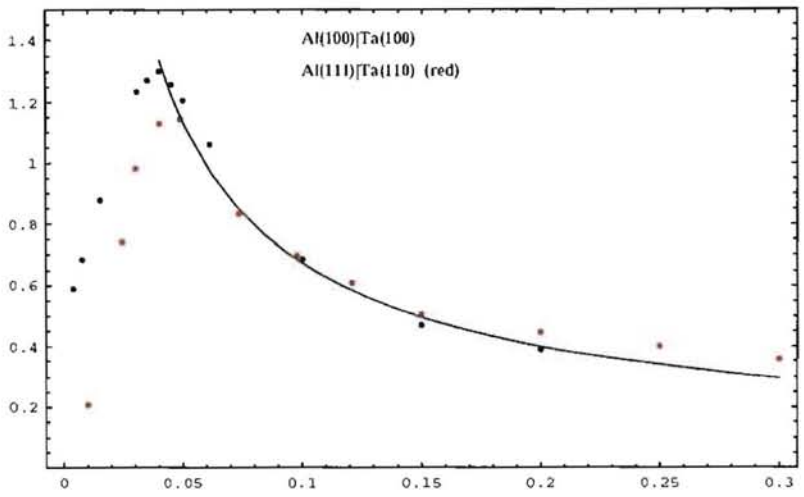


Ta/Al (15 GPa)

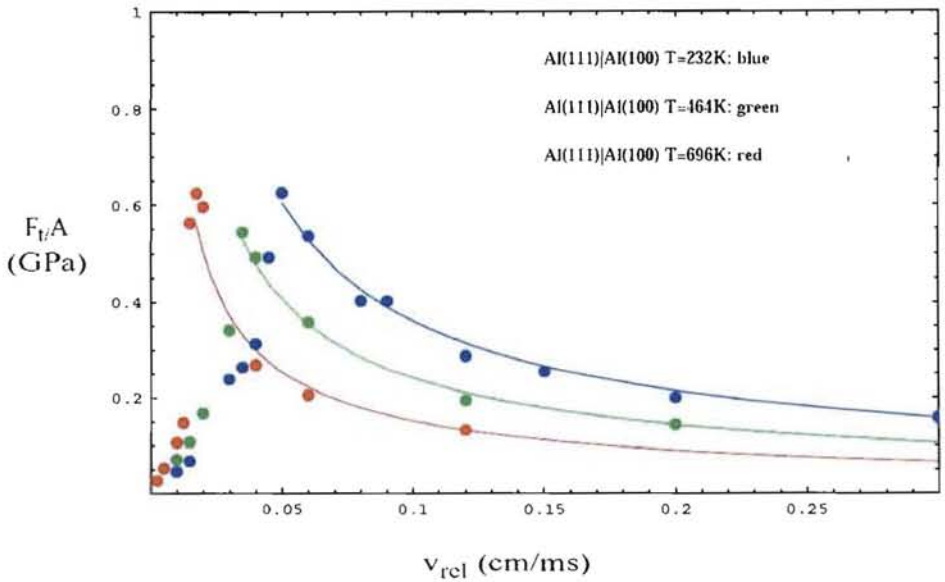

# Velocity Dependence: Four regimes of characteristic dissipation

**There are four regions in velocity that correspond to different dominant modes of dissipation.**

1. **0-0.5 $v_c$ : anharmonic phonon dissipation**
2. **0.5-1.0 $v_c$ : plastic deformation**
3. **1.0-2.0 $v_c$ : structural transformation**
4. **$v > 2.0\ v_c$ : fluidization**

# Velocity Dependence: Anharmonic phonon dissipation

## Low velocity regime

In this regime ($v \ll v_c$), exact results are possible and the dissipation is due to anharmonic phonons:

$$\delta F_{12} = \frac{2\pi}{\Omega^2}\sum_{\vec{q}}(\vec{q}\cdot\hat{t})|\phi(\vec{q})|^2\int[\ S_1(\vec{q},-\vec{q};\omega)ImG_2^{ret}(\vec{q},-\vec{q};\omega+\omega_0(\vec{q}))$$
$$+ S_2(\overrightarrow{-q},\vec{q};\omega)ImG_1^{ret}(\vec{q},-\vec{q};\omega+\omega_0(\vec{q}))\ ]d\omega$$

where $\omega_0(\vec{q}) = \vec{q}\cdot v$. When v approaches zero the rhs is linear in $\omega_0(\vec{q})$. $S_1(\vec{q},-\vec{q};\omega)$ is a dynamic structure factor defined by

$$S_1(\vec{q},-\vec{q}';t-t') = \langle n_1(\vec{q},t)n_1(\overrightarrow{-q'},t')\rangle_0 = \sum_{\substack{i\in\Omega_1\\ j\in\Omega_1}} Tr\rho_0 e^{i\vec{q}\cdot R_i(t)}e^{-i\vec{q}'\cdot R_j(t')}$$

and $ImG_1^{ret}(\vec{q},-\vec{q};\omega+\omega_0(\vec{q}))$ is the density-density response function written as the imaginary part of the Green's function.

For an incommensurate interface thes expressions lead to a linear velocity dependence at low velocities proportional to inverse phonon lifetimes from evaluation of the imaginary part of the retarded phonon Green's function.

# Velocity Dependence: Plastic Deformation

**Intermediate regime ($0.5v_c \le v \le v_c$): Plasticity**

**Al/Al stacking fault formation at $v_{rel}$=150 m/s, $T_{res}$=696 K**

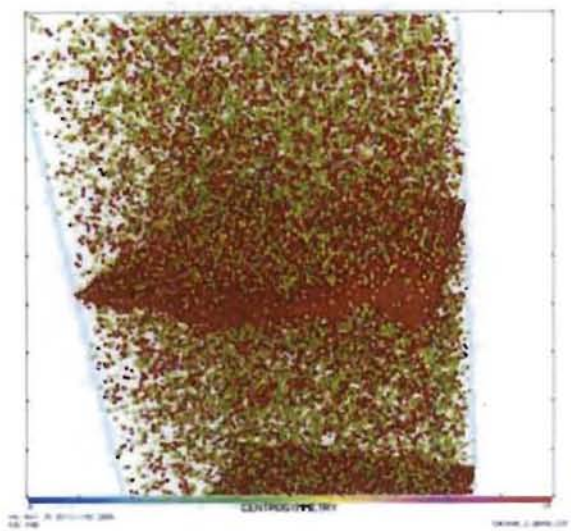

**t=0.265 ns**

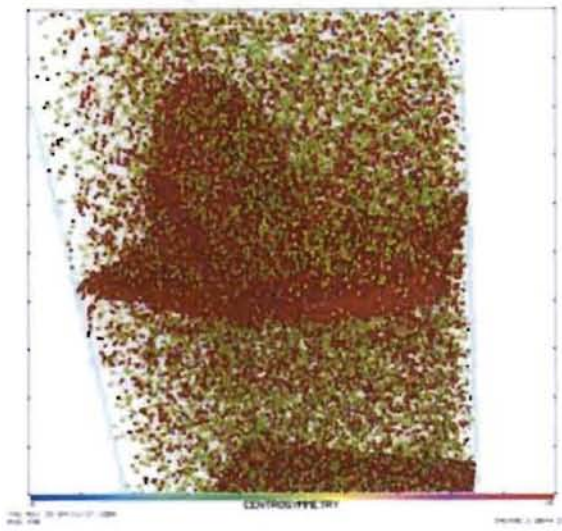

**t=0.269 ns**

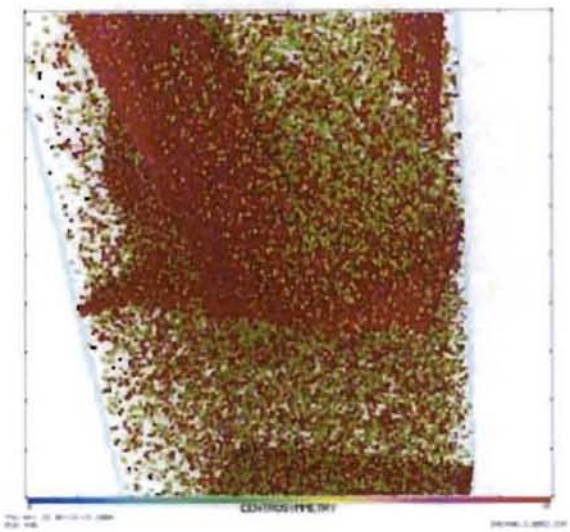

**t=0.277 ns**

# Velocity Dependence: Structural Transformation

Cu(2D) P=30GPa, v- 0.12c, Mechanical Mixing

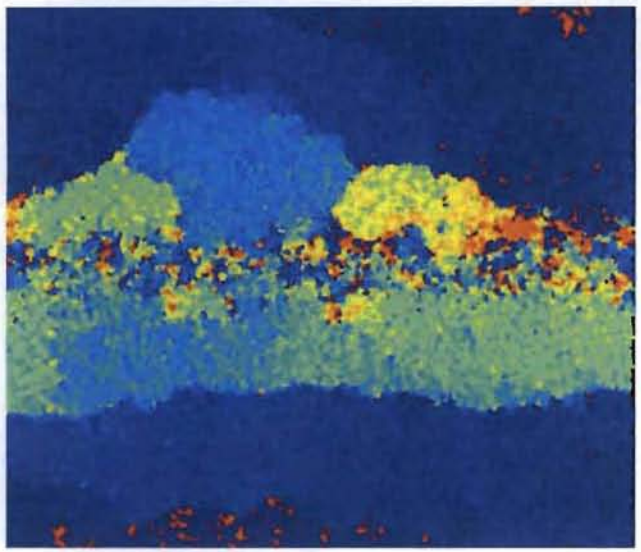

Cu(2D) Grain Structure

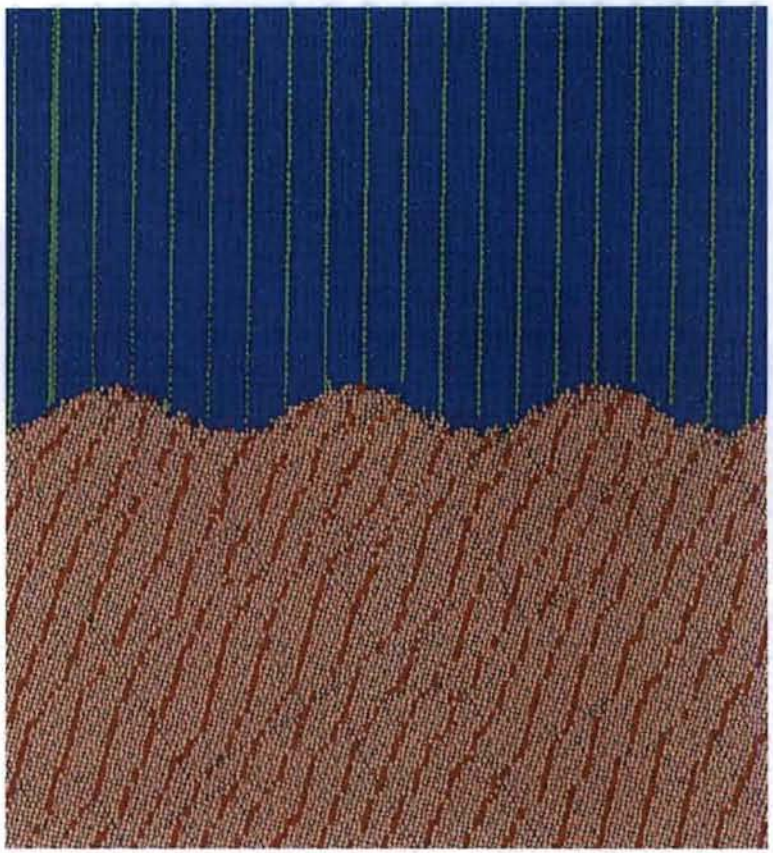

Cu/Ag
P=5.1 GPa v=470 m/s

# Velocity Dependence: Structural Transformation - Fluidization

- **Al(111)/Al(001) Interface at very high velocities exhibits confined non laminar Couette fluid flow behavior**

Tangential Velocity Field ($v_x(x,y)$)

$V_{rel}$= 2 km/s, $T_{Res}$=696, 464, 232 K°

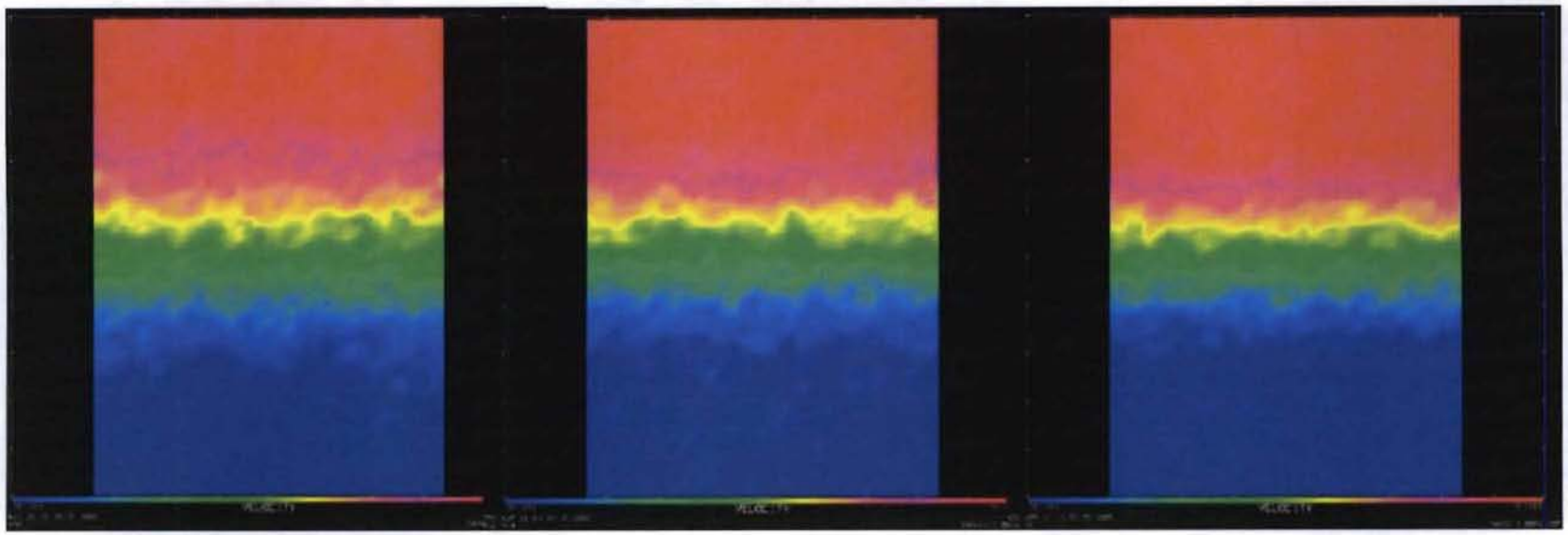

T=696 °K T= 464 °K T= 232 °K

# Fluidization : Tangential Velocity Profile - Al/Al

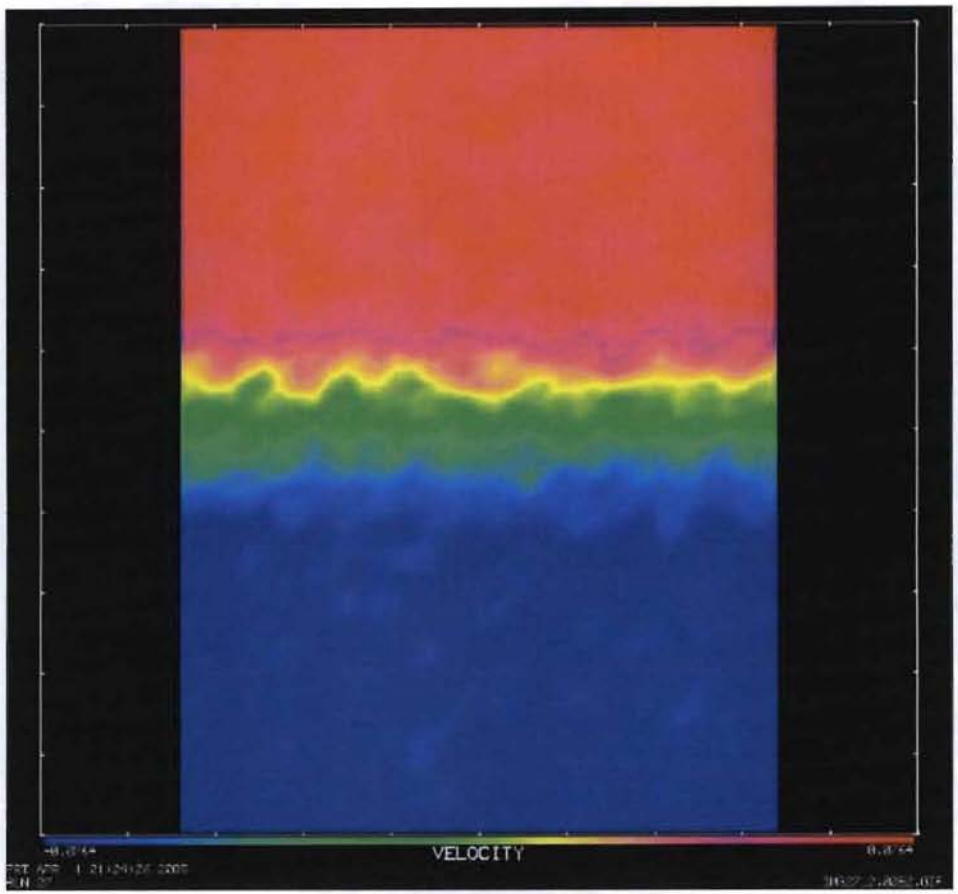


**Al(111)/Al(001) $V_x(x,y)$ for $v_{rel}$ = 1.5 km/s, P=15 GPa**

# Velocity Dependence: Structural Transformation - Fluidization

- Al(111)/Al(001) Interface at very high velocities-particle positions: Couette region size depends on boundary temperature.

**Particle Positions (001) plane - sample center**

$V_{rel}$ = 2.0 km/s, $T_{Res}$=696, 464, 232 K°

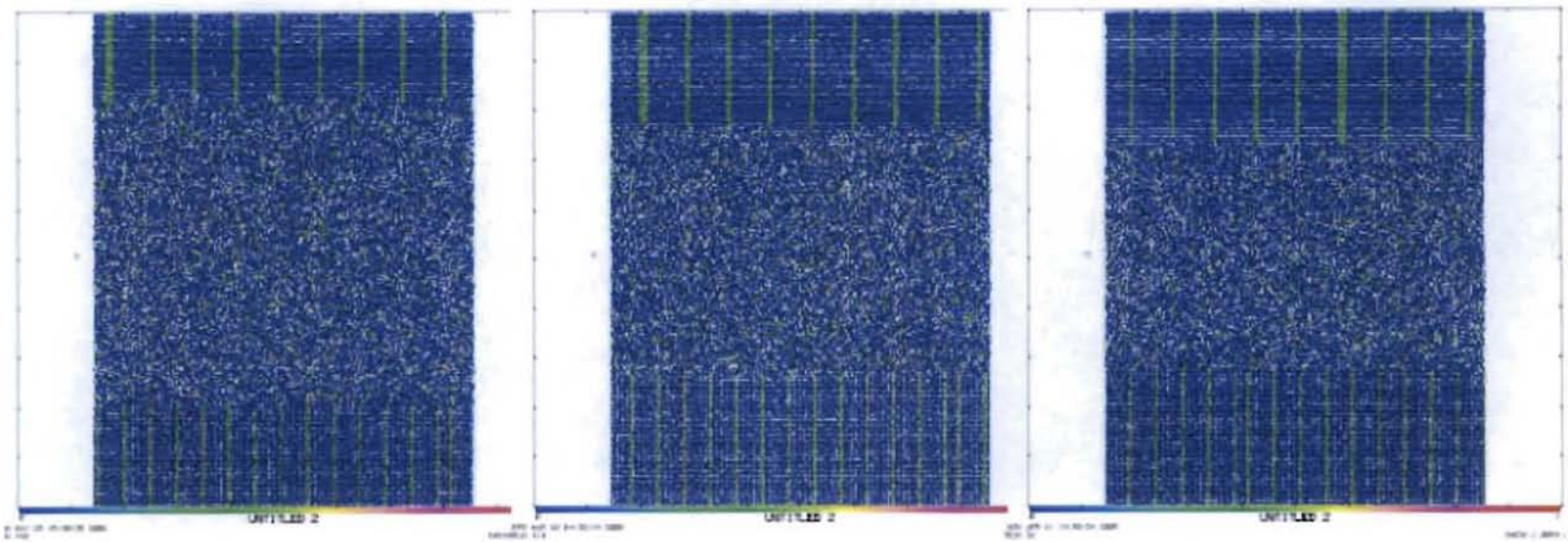

T=696 °K  T= 464 °K  T= 232 °K

# Fluidization : Particle Positions - Al/Al

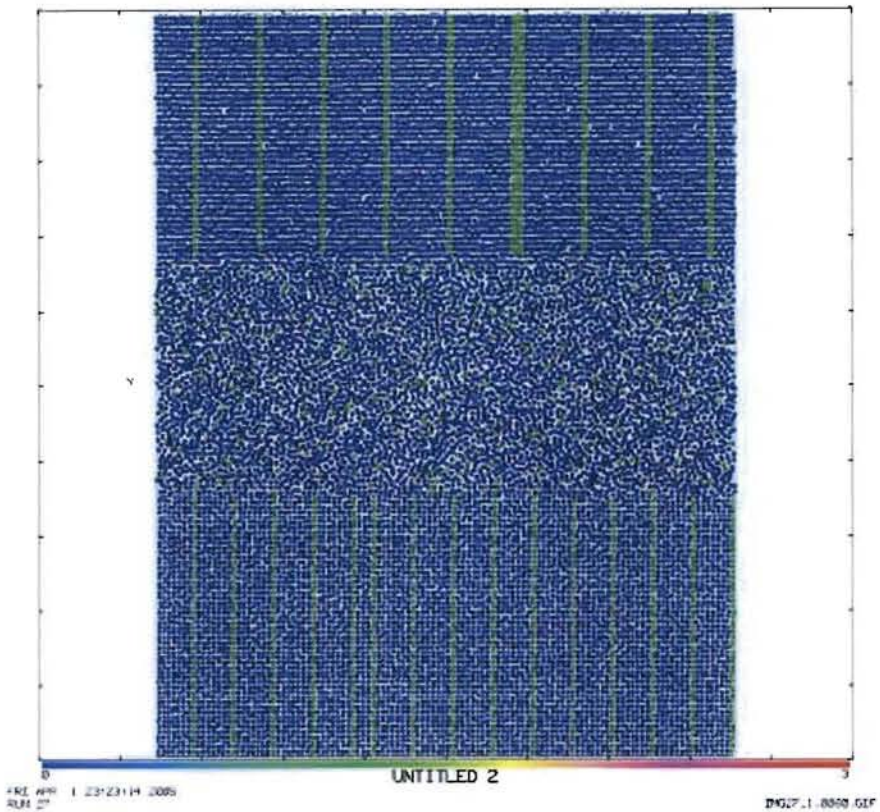


**Particle Positions (001) plane - sample center**

$v_{rel}$ = 1.5 km/s

# NEMD Simulations - Summary

- NEMD simulations have shown velocity weakening at high velocities for a variety of metal/metal interfaces.
- There are four regimes of deformation as velocity increases: anharmonic phonon dominated, dislocation and defect dominated, structural transformation, and fluidization.
- Material mixing occurs at the higher velocities.
- The above are qualitatively similar to the experimental picture described above.
- The velocity dependence at high velocities is well represented by a power law velocity dependence for the frictional force.

# Generic properties of the velocity dependence of the frictional force and analysis

- **Al(111)/Al(001) results have shown scaling behavior:**

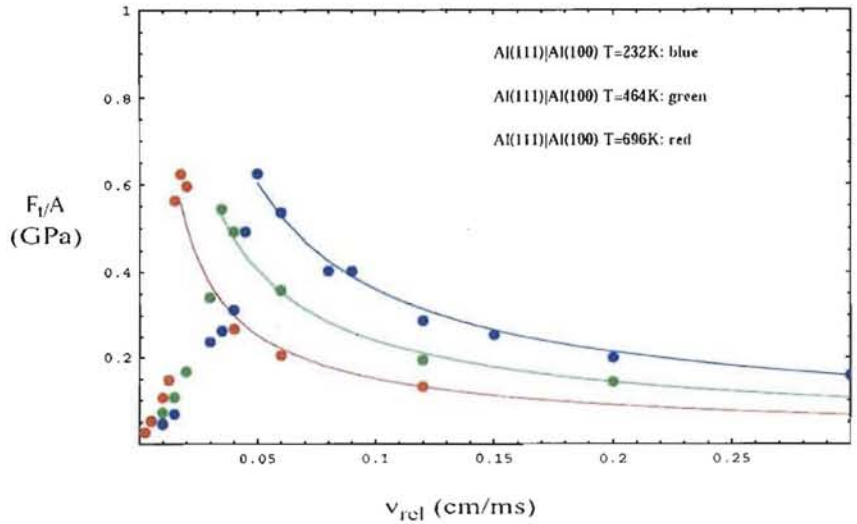


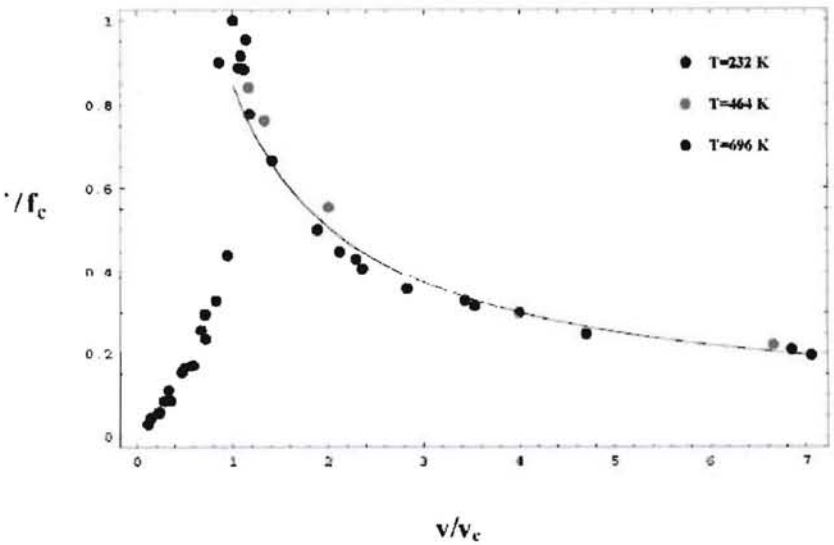


**P=15 GPa, $N_{atoms}$=1.5 $10^6$**

# The simulation results are well represented by a scaled function for the tangential force per unit area

$$f \equiv \frac{F}{A} = f_c \left( \frac{v}{v_c} \right)^{-\beta}$$

$$v_c = \frac{4 \bar{\kappa} T^*}{f_c L} \left( 1 - \frac{T_0}{T^*} \right)$$

- $T^*$ is a critical temperature at $v_c$ and $\bar{\kappa}$ is an average thermal conductivity. $T^* \simeq T_{melt}$ and $T_0$ is the boundary temperature.

$$\bar{\kappa} = \frac{1}{\left( T^* - T_0 \right)} \int_{T_0}^{T^*} \kappa(T) dT$$

# Scaling of the Frictional Force – Al/Al (Cont.)

**The temperature dependence of $v_c$ is very nearly linear with respect reservoir temperture**

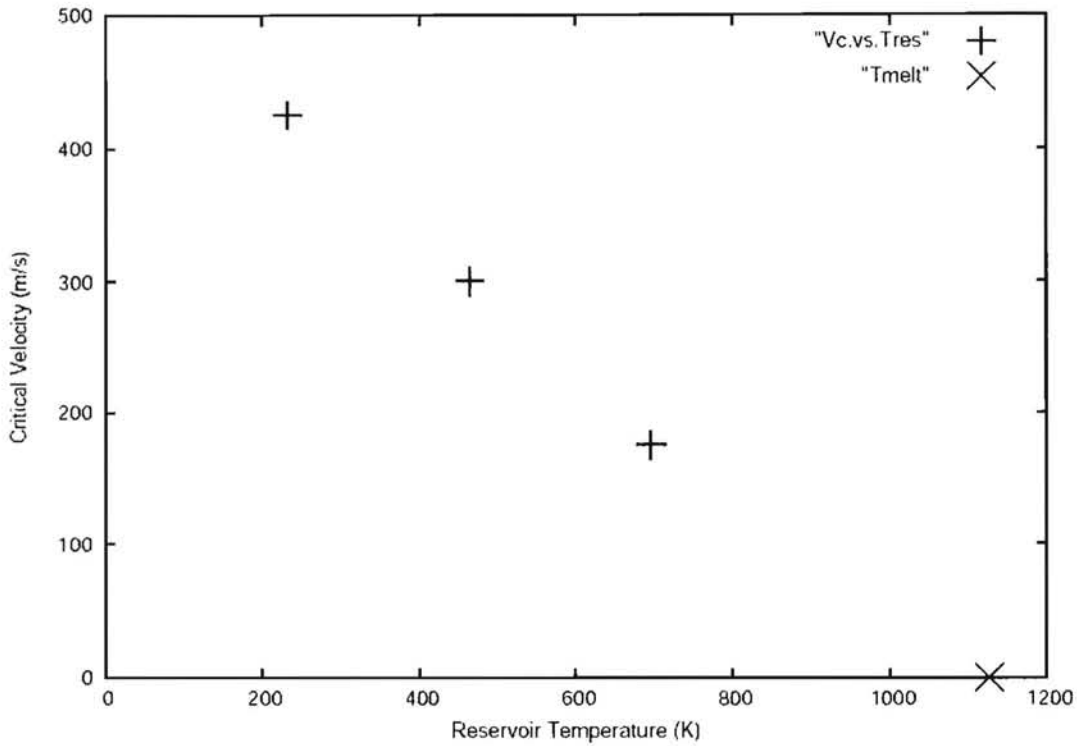

# Structural transformation for $v_c<v<v_{c1}$

- For velocities $v_c<v<v_{c1}$, a transformation front coincident with the sliding surface forms, transforming (111) material into (001) material.

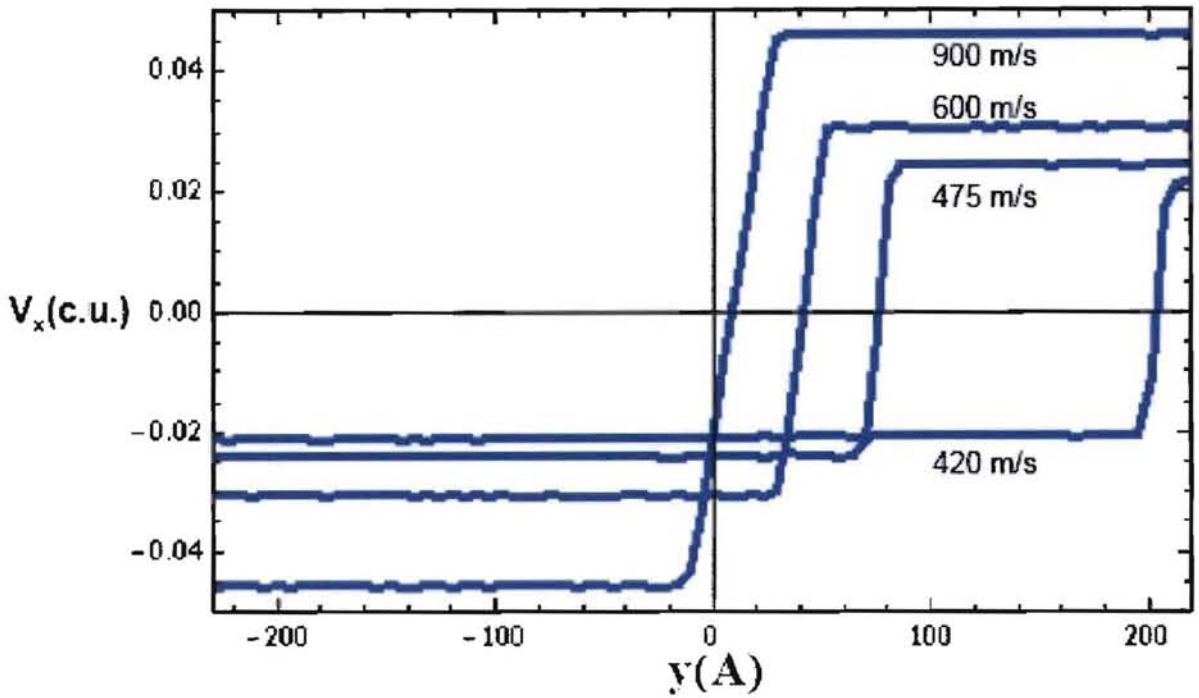

# For velocities above $v_{c1}$ a Couette flow pattern forms characterized by a critical strain rate.

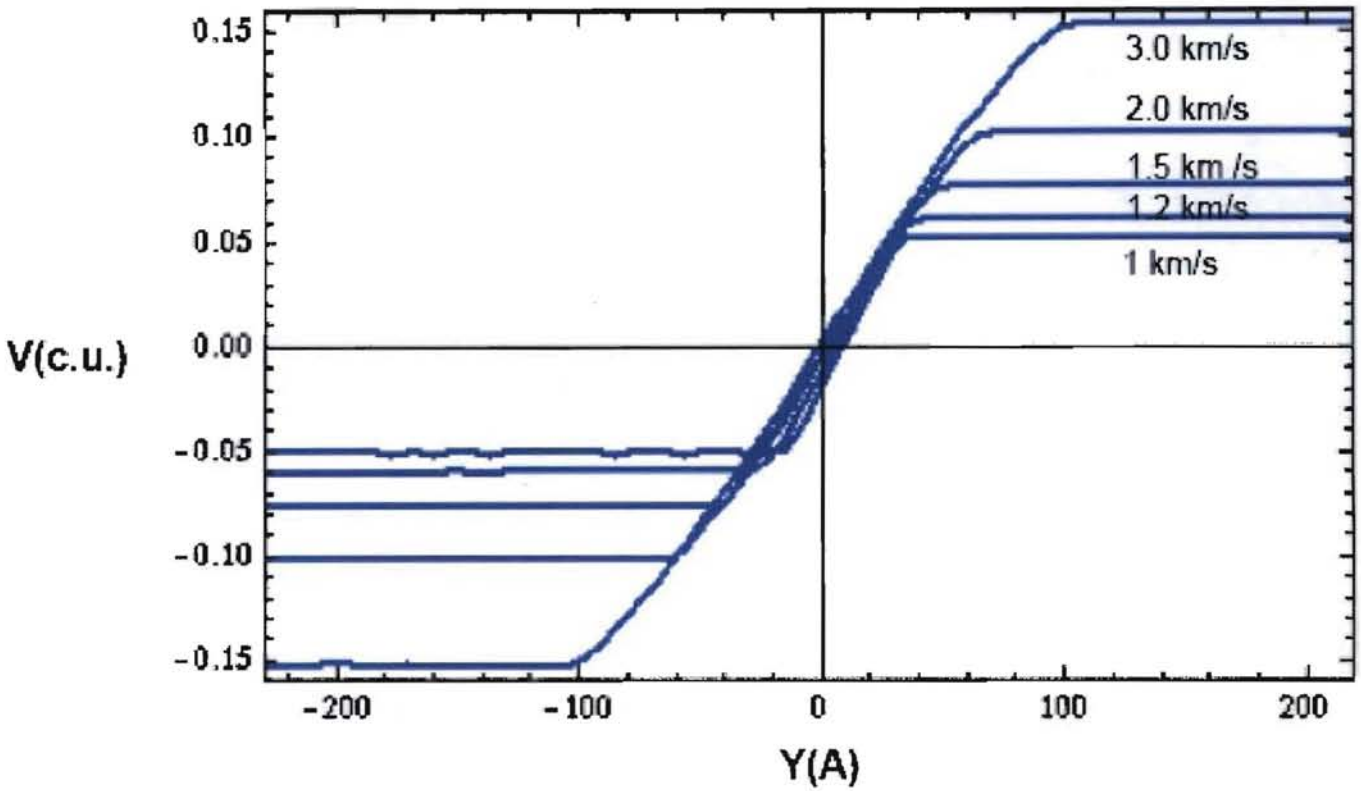


$T_0 = 232$ K

# The critical strain rate depends on the boundary temperature and the temperature profile is parabolic in the fluid region.

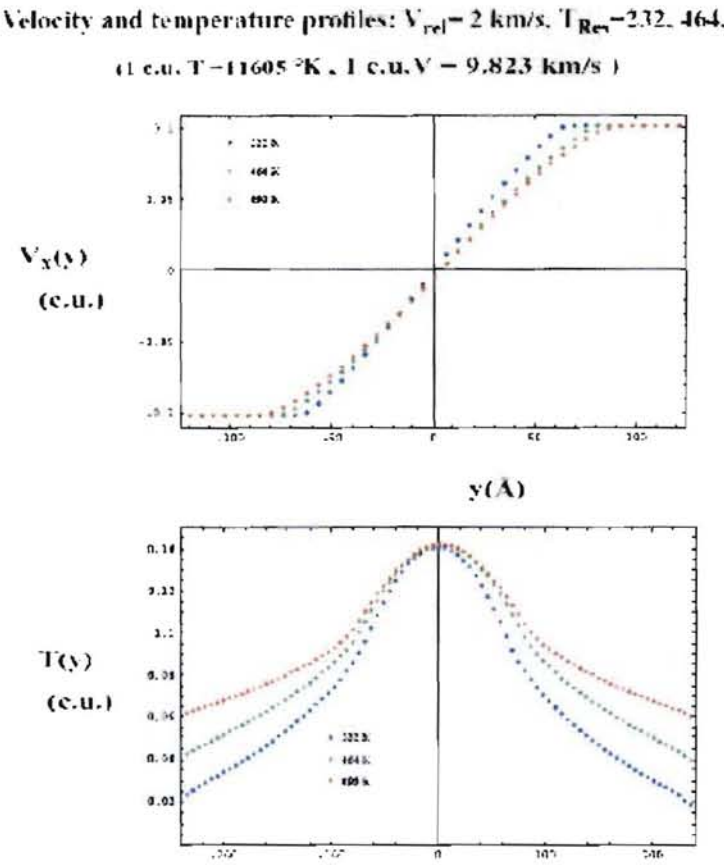

# The velocity dependence of the interface temperature in the high velocity regime may be analyzed in terms of fluid and mechanical quantities

$$T(0) = T_m + \frac{1}{8}\left\langle \frac{\kappa}{\eta} \right\rangle^{-1} v^2$$

$$T(0) = T_m + \frac{1}{8}\left\langle \frac{c_v}{Pr} \right\rangle^{-1} v^2$$

$$T(0) = T_m + \frac{1}{8}\left[ \frac{f}{\langle \kappa \rangle \dot{\varepsilon}_c} \right] v^2$$

$$T(y) = T(0) - \frac{1}{2}\left\langle \frac{\kappa}{\eta} \right\rangle^{-1} \dot{\varepsilon}_c^2 y^2$$

where $\dot{\varepsilon}_c$ is the critical strain rate in the Couette regime, $\kappa$ is the thermal conductivity, $\eta$ is the fluid viscosity, $c_V$ the specific heat and Pr the Prandt'l number and the brackets denote thermal averages between T(0) and $T_m$ and between T(0) and T(y) in the last equation.

[J.E. Hammerberg, B.L. Holian, T.C. Germann and R. Ravelo, 2009, "High Velocity Properties of the Dynamic Frictonal Force between Ductile Metals", Proc. Shock Compression of Shock Compression of Condensed Matter-2009.]

# These relations and the scaled form for F imply relationships for T(0) and the critical strain rate.

$$T(0) = T_m + \frac{1}{8}\left[\frac{f_c v_c^{\beta}}{\langle\kappa\rangle \dot{\varepsilon}_c}\right] v^{1+\alpha} \qquad (\alpha = 1-\beta)$$

$$\dot{\varepsilon}_c = A \frac{f_c}{\langle\kappa\rangle} v_c^{\beta}$$

where the second expression assumes the result from the NEMD simulations which show the values for T(0) independent of $v_c$ in the Couette regime.

# Couette flow regime

**From these expressions it follows that the velocity dependence of T(0) apart from the temperature dependence of $\kappa$ is $v^{1+\alpha}$. The expression for T(0) may also be solved for $\kappa$:**

| V(km/s) | T(0) (K) | $\kappa$ (W/(m-K) |
|---|---|---|
| 0.8 | 1220 | 1.94 |
| 0.9 | 1277 | 1.39 |
| 1.2 | 1353 | 1.32 |
| 1.5 | 460 | 1.19 |
| 2.0 | 1694 | 1.00 |
| 3.0 | 2089 | 0.98 |

# Couette flow regime

**There is also a relationship between $v_c$ and $v_{c1}$**

$$\frac{v_{c1}}{v_c} = \left(\frac{\eta(T_m)\dot{\varepsilon}_c}{f_c}\right)^{-\frac{1}{\beta}}$$

# Summary

- The tangential force between ductile metals exhibits a generic velocity dependence.
- There is a critical velocity, $\mathbf{v_c}$ beyond which the tangential force decreases and the dominant dissipative mechanism changes from plastic deformation to structural transformation and fluidization at the highest velocities.
- There is a second critical velocity, $\mathbf{v_{c1}} > \mathbf{v_c}$, beyond which the fluid interface exhibits Couette flow. In this regime the tangential force is determined by a critical strain rate, the fluid viscosity and thermal conductivity.
- The tangential force for $v > \mathbf{v_c}$ exhibits scaling behavior with a power law exponent, $\beta = 3/4$, and $f \sim (v/v_c)^{-\beta}$.
- For $v > v_{c1}$ , the flow is non-laminar and mixing.

# Summary

- Ultimately one would like to have a constitutive model for the tangential force to be used in macroscopic engineering simulation computer models:

$$\frac{F_t}{A} = f(P, T; \varepsilon_p, v_{rel})$$

where A is surface area, P pressure, T temperature, $\varepsilon_p$ plastic strain, and $v_{rel}$ the relative velocity. The above expressions are the basis for such a model.